Design of Wide-Band Tunable Optical Filters with Cascaded Microring Resonators and Shaped-Finger Comb-Drive Actuators

Dooyoung Hah
Department of Electrical and Electronics Engineering
Abdullah Gül University
Kayseri, Turkey
dooyoung.hah@agu.edu.tr

***Abstract*—Utilizing the Vernier effect, series coupling of multiple microring resonators with different sizes is used to design a wide-band (free spectral range: 36 nm) tunable filter. For index modulators that shift the filter spectrum by changing effective indices through evanescent coupling, silicon waveguides are considered, which make the fabrication simpler. Effects of the index modulator width to the filter characteristics are studied. A narrower modulator (width: 50 nm) does not incur much loss to the resonator, but requires hopping among several bands since its tuning effect is moderate. On the other hand, a wider modulator (width: 100 nm) can cover the full free spectral range without band hopping, but induces severe loss when it is close to the resonator. The shaped-finger comb-drive actuator design method is applied to obtain linear drop channel control.**

Keywords—microring resonator; tunable optical filter; comb-drive actuator; Vernier effect; shaped finger

I. INTRODUCTION

A microring resonator is one of the essential components that constitute optical filters in photonic integrated circuits (PICs). The filter characteristics, therefore, often heavily depend on those of the microring resonators. For example, the tunable range of a filter is limited by the free spectral range (FSR) of the resonator. An FSR of a microring resonator is inversely proportional to the length of its perimeter. And hence, in order to design a wide-band filter with a single resonator, the resonator has to have a small radius. For instance, to cover the entire C-band (1530-1565 nm) in dense wavelength division multiplexing (DWDM), a microring resonator made of silicon waveguide has to have a radius smaller than 3 μm. There are a few issues with this small a radius for a ring resonator. First, optical loss occurred in a resonator due to scattering and junction mismatch increases drastically as the radius of curvature is reduced, which degrades the quality factor of the resonator [1]. Second, as the resonator size shrinks, although the FSR becomes wider, tuning itself becomes more difficult because the length of the light path available for tuning—whichever tuning method is used, whether it is thermo-optic, free carrier injection, or evanescent coupling—is reduced. Therefore, a different approach is needed for wide-band tuning in optical filters other than reducing the size of the resonator, and one such approach explored by several research groups recently is utilization of the Vernier effect that employs cascaded microring resonators [2-6].

Series or parallel coupling of multiple resonators is one of the typical methods employed in filter design for improved filter characteristics such as a box-shape pass-band. Such coupling among resonators of different sizes results in the so-called Vernier effect by which the tuning range of the filter is extended as illustrated in Figs. 1 and 2. When resonators of two different FSRs are coupled together, the FSR of the combined filter can be extended by several times—the FSR of the cascaded resonators becomes the least common multiple of the FSRs of the individual resonators. In this work, a resonator with an FSR of 12 nm and one with an FSR of 9 nm are cascaded in series to result in a filter with an FSR of 36 nm. The perimeters of the resonators (silicon, width: 200 nm) designed for such FSRs in C-band are 55.1 μm and 73.4 μm. With this extension of possible tuning range at hand, the filter design will be described in detail.

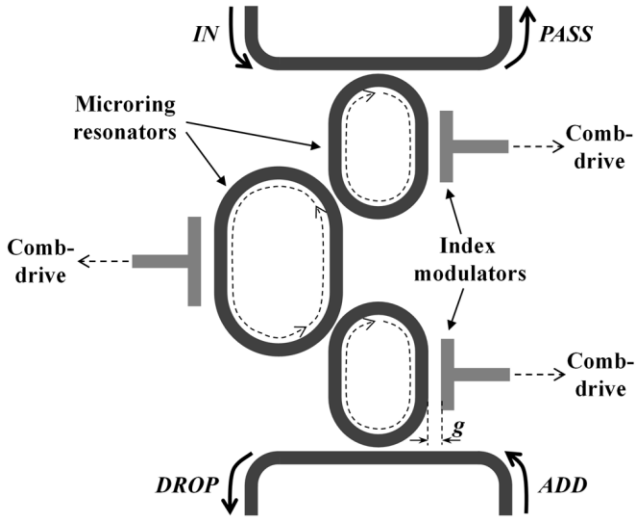

Fig. 1. Schematic diagram of a wide-band tunable optical filter with cascaded resonators and micromechanical actuators. Top view.

This work was supported by Research Fund of the Abdullah Gül University (Project Number: FOA-2016-49).

978-1-5090-1457-6/16/$31.00 ©2016 IEEE

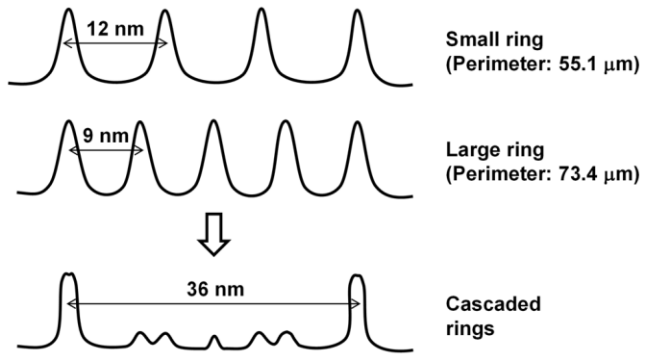

Fig. 2. Principle of free spectral range (FSR) expansion in a filter with cascaded microring resonators using the Vernier effect. Output spectra at the *DROP* port.

II. Cascaded Microring Resonators

In terms of the tuning mechanism, mechanical tuning is considered for its minimal standing power consumption characteristics [7-10]. In this mechanism, an index modulator which is placed closely to the resonator induces evanescent coupling, altering the effective indices of the modes propagating through the resonator. The optical power entering the *IN* port (see Fig. 1) is coupled to the resonators, and at resonance, most of it excluding the loss comes out of the *DROP* port. When the wavelength is off the resonance, most of the input power is passed to the *PASS* port. The optical power at the *DROP* port, P_{DROP} can be expressed as,

$$P_{DROP} = \left| \frac{\alpha_{msb\_sr}\sqrt{\alpha_{msb\_lr}}\left(1-|t_{rr}|^2\right)\left(1-|t_{br}|^2\right)}{\left(1-C_1 t_{rr}-C_2 t_{rr}^* + C_1 C_2\right)\left(1-C_1 D\right)} a_{in} \right|^2, \quad (1)$$

where

$$C_1 = \alpha_{msb\_sr}\alpha_{im\_sr}\exp\left(-j\phi_{1r\_sr}\right)t_{br}^*, \quad (2a)$$

$$C_2 = \alpha_{msb\_lr}\alpha_{im\_lr}\exp\left(-j\phi_{1r\_lr}\right)t_{rr}^*, \quad (2b)$$

$$D = \frac{|t_{rr}|^2 - C_1 t_{rr}|t_{rr}|^2 - C_2 t_{rr}^* + C_1 C_2}{t_{rr}^* - C_1|t_{rr}|^2 - C_2\left(t_{rr}^*\right)^2 + C_1 C_2 t_{rr}^*}. \quad (2c)$$

a_{in}, t_{rr}, and t_{br} are the input field amplitude, transmission coefficient between the resonators, and transmission coefficient between a bus waveguide and a small ring resonator, respectively. α_{msb_sr} and α_{msb_lr} are unloaded (material, scattering, and bending) loss of a small ring resonator and of a large ring resonator, respectively. α_{im_sr} and α_{im_lr} are loss caused by evanescent coupling to the index modulator in a small ring resonator and in a large ring resonator, respectively, which depend on the gap (g) between the resonator and the index modulator. ϕ_{1r_sr} and ϕ_{1r_lr} are phase shifts incurred during one round trip in a small ring resonator and in a large ring resonator, respectively, which also include the additional phase shifts caused by evanescent coupling to the index modulators, again functions of g.

In the author's previous work [7], a material with a low refractive index (n = 2.2) was considered for an index modulator for its low power coupling characteristics. In this work, a silicon index modulator (n = 3.48) is considered, which bears an advantage of simpler fabrication processes because all the structures can be made out of the same material. Since high refractive index of the modulator incurs high coupling loss (α_{im}), the modulator was designed with narrower width—two different values of 50 nm and 100 nm were considered in this work. A narrower index modulator does not incur substantial coupling loss, but its range of continuous wavelength tuning is limited so that tuning of a full FSR has to be realized by stitching of tuning in multiple bands, which will be described later. A wider index modulator can perform full-FSR tuning within one band, however it can result in substantial coupling loss.

Fig. 3 shows the calculated resonant wavelengths (λ_r) of the single-resonator filters with respect to the gap (g) between the resonator and the index modulator, for two different perimeters

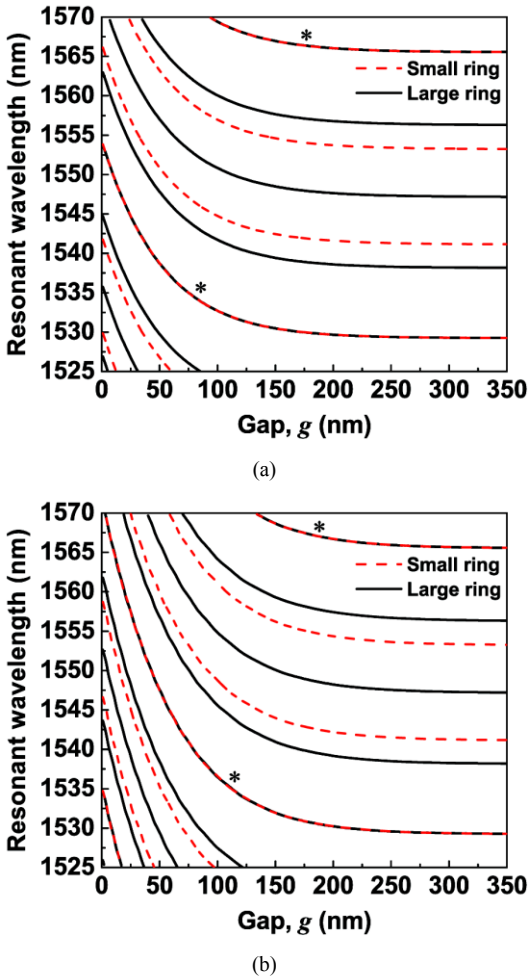

Fig. 3. Calculated resonant wavelengths of single-resonator filters, with respect to the gap g between the resonator and the silicon index modulator. Perimeter: small ring – 55.1 μm, large ring – 73.4 μm. Curves marked with *: spectra coincide for a small ring resonator and a large ring resonator. Width of the index modulator w_{im}: (a) 50 nm, and (b) 100 nm.

(55.1 μm and 73.4 μm) and two different index modulator widths (50 nm and 100 nm). The ring perimeters were chosen so that their resonant wavelengths coincide at both ends of the extended FSR of the cascaded filter. This can be seen from the curves indicated by * in Fig. 3. The major effect of the index modulator width is the tunability. In the case of the 100-nm-wide modulator, the full FSR from 1529 nm to 1565 nm can be covered (see the bottom curve that is marked by * in Fig. 3b). Therefore, identical modulator gaps can be used for both of the rings for tuning, as can be seen from Fig. 4(b). Fig. 4 shows the spectra of the cascaded-resonator filter at the *DROP* port, calculated at various index modulator gaps (g) using (1). However, in the case of the 50-nm-wide modulator, the entire FSR cannot be covered in band. Therefore, it has to be covered by moving from band to band. This "band hopping" is used to produce Fig. 4(a), and as a result, the required modulator gaps are different between two rings, especially for longer wavelengths. In either case, the results show that the entire FSR can be tuned with the designed filter. The calculated spectra also show another effect of index modulator widths, i.e. the coupling losses—the device with 100-nm-wide modulator shows significant coupling loss compared to the one with 50 nm.

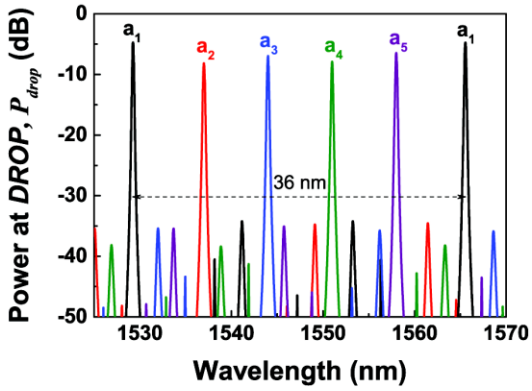

(a)

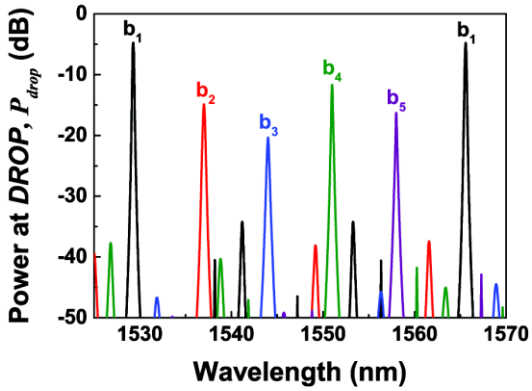

(b)

Fig. 4. Calculated spectra of cascaded-resonator filters at the *DROP* port (P_{drop}) for various index modulator positions (or gaps g). (a) Width of the index modulator w_{im}: 50 nm. g for the small ring/large ring are a_1: 350 nm/350 nm, a_2: 60 nm/60 nm, a_3: 111 nm/75 nm, a_4: 49 nm/98 nm, and a_5: 88 nm/45 nm, respectively. (b) w_{im}: 100 nm. g for both of the rings are b_1: 350 nm, b_2: 97 nm, b_3: 62 nm, b_4: 40 nm, and b_5: 24 nm.

III. Actuator Design

The translation of the index modulators are controlled by comb-drive actuators. The control becomes a bit more complicated especially in the case of the narrow index modulator because it involves band hopping as can be learned from Fig. 3(a). If typical comb-drive actuators with straight fingers are used, the control can become quite challenging due to high nonlinearity of the wavelength-voltage (λ_r-V) characteristics [11]. This challenge can be substantially alleviated by employing a shaped comb finger design which was proposed by the author [11, 12]. By adopting a biasing scheme that reverses the sign of the convexity of the g-V curve, and by obtaining an approximated solution to the governing differential equation given below, a linear λ_r-V characteristic curve can be achieved [11].

$$d'_{bias}(x) = \frac{1}{x - \dfrac{(d_{max}+d_{min})d_{min}x_{max}}{[d_{bias}(x)]^2}} \times \left[d_{max}+d_{min}-d_{bias}(x)+\frac{2\varepsilon_0 a_1 \lambda_r'(x)}{C_0}V(x)\right] \tag{3}$$

$$V(x) = \sqrt{\frac{d_{max}+d_{min}-d_{bias}(x)}{\varepsilon_0 a_1}\left[\frac{d_{min}x_{max}}{d_{bias}(x)}-x\right]} \tag{4}$$

$$d_{ctrl}(u) = -d_{bias}(x_{\max}-u)+d_{max}+d_{min} \tag{5}$$

ε_0, a_1, and C_0 are vacuum permittivity, a comb-drive actuator parameter determined by its geometrical dimensions, and a linear constant of λ_r-V relationships, respectively. $\lambda_r(x)$ is obtained from Fig. 3 for each resonator. Other parameters are defined in Fig. 5.

The said design method was applied for the current cascaded-resonator filter. Fig. 6 shows the calculated finger gaps of the comb-drive actuators in the case of the 50-nm-wide index modulator, for both small and large microring resonators. In the case of the 100-nm-wide index modulator, the finger shapes are equal between the small and the large microring resonators because they require the same V-x relationships. Fig. 7 shows the calculated V-λ_r characteristics for both of the index modulator widths. In the case of the 100-nm-wide index modulator (Fig. 7b), the channel selection is straightforward because of the same λ_r-V relationships shared by the small and the large resonators. In the 50-nm-wide index modulator case, because of difference in the λ_r-V relationships between the small and the large resonators, a set of two voltages has to be chosen from Fig. 7(a) to select a drop channel. For example, to select a channel with the center wavelength of 1543 nm, the control voltages are to be selected as 4.6 V for the small resonator and 2.5 V for the large resonator. It is demonstrated that in both cases of index modulator widths, a linear control

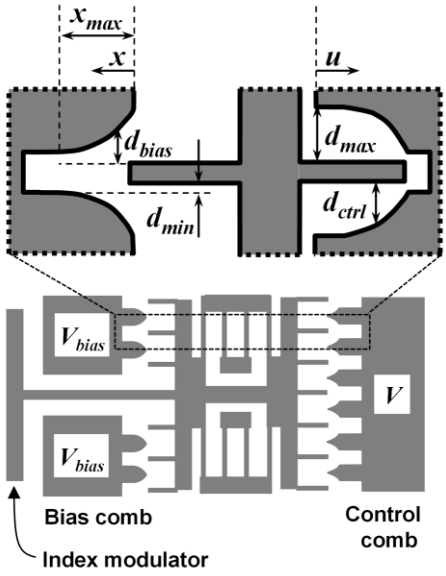

Fig. 5. A schematic drawing of a shaped-finger comb-drive actuator.

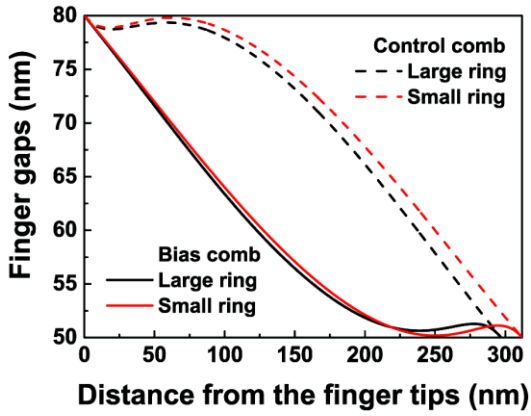

Fig. 6. Calculated finger gaps (d_{bias} and d_{ctrl}) for linear wavelength-voltage relationships in a filter with cascaded microring resonators. Width of the index modulator w_{im}: 50 nm.

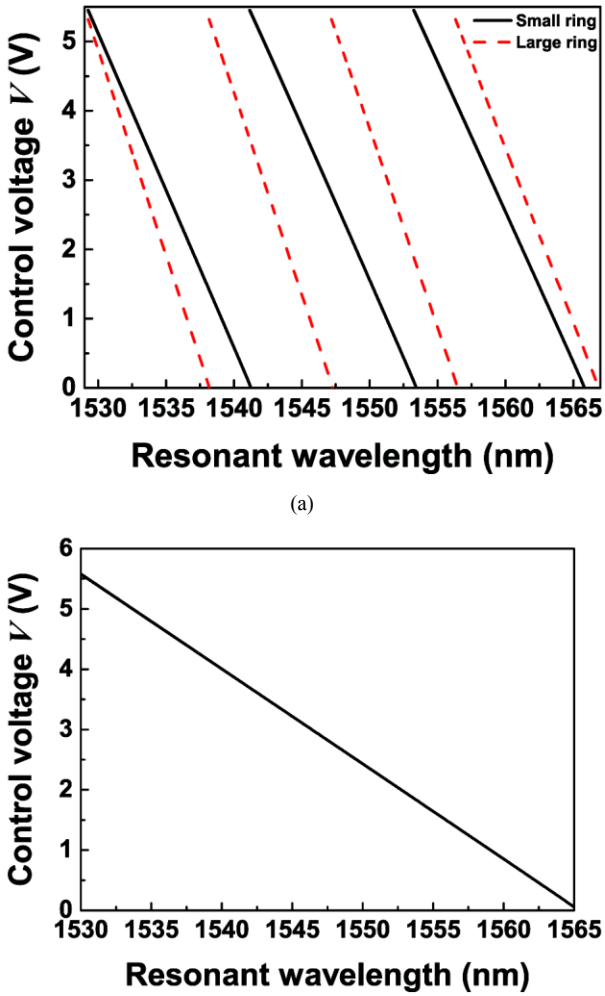

Fig. 7. Calculated voltage-wavelength relationships (V-λ_r) for filters with cascaded microring resonators. Design parameters: number of fingers = 50, spring constant = 0.27 N/m, and thickness of a finger = 200 nm. Width of the index modulator w_{im}: (a) 50 nm, and (b) 100 nm.

can be achieved. In the case of 50-nm-wide index modulator, because of this linear control, hopping between different sections of the band can be more easily manipulated. It should be noted that although λ_r-g characteristics of the two individual ring resonators coincide at the both ends of the filter FSR, their corresponding λ_r-V characteristics are designed differently from each other because their individual FSRs, and hence their tuning ranges within one section of the band are different from each other as can be seen in Fig. 7(a). In the case of the small resonator, the gap (g) change should be at least from 350 nm to 38 nm to cover its FSR. In the large resonator case, it should be from 350 nm to 53 nm.

IV. Conclusions

36-nm-FSR band-pass optical filters were designed for the C band by cascading multiple microring resonators based on the Vernier effect. Mechanical tuning of the cascaded filter with the silicon index modulators was confirmed through simulation. Trade-off between the continuous tuning range and the evanescent coupling loss with respect to the width of the index modulator was discussed. Shaped comb finger design was applied to the cascaded filter for linear drop channel control.

References

[1] V. Van, P. P. Absil, J. V. Hryniewicz, and P.-T. Ho, "Propagation loss in single-mode GaAs–AlGaAs microring resonators: measurement and model," J. Lightwave Technol., vol. 19, pp. 1734-1739, 2001.

[2] Y. Yanagase, S. Suzuki, Y. Kokubun, and S. T. Chu, "Box-like filter response and expansion of FSR by a vertically triple coupled microring resonator filter," J. Lightwave Technol., vol. 20, pp. 1525-1529, 2002.

[3] A. Melloni and M. Martinelli, "Synthesis of direct-coupled-resonators bandpass filters for WDM systems," J. Lightwave Technol., vol. 20, pp. 296-303, 2002.

[4] R. Grover, at al., "Parallel-cascaded semiconductor microring resonators for high-order and wide-FSR filters," J. Lightwave Technol., vol. 20, pp. 900-905, 2002.

[5] S. J. Choi, Z. Peng, Q. Yang, S. J. Choi, and P. D. Dapkus, "Tunable narrow linewidth all-buried heterostructure ring resonator filters using Vernier effects," Photon. Technol. Lett., vol. 17, pp. 206-208, 2005.

[6] P. Prabhathan, Z. Jing, V. M. Murukeshan, Z. Huijuan, and C. Shiyi, "Discrete and fine wavelength tunable thermo-optic WSS for low power consumption C+L band tunability," Photon. Technol. Lett., vol. 24, pp. 152-154, 2012.

[7] D. Hah, J. Bordelon, and D. Zhang, "Mechanically tunable optical filters with a microring resonator," Applied Opt., vol. 50, pp. 4320-4327, 2011.

[8] L. J. Kauppinen et al., "Micromechanically tuned ring resonator in silicon on insulator," Optics Lett., vol. 36, pp. 1047-1049, 2011.

[9] T. Ikeda and K. Hane, "A microelectromechanically tunable microring resonator composed of freestanding silicon photonic waveguide couplers," Appl. Phys. Lett., vol. 102, 221113, 2013.

[10] H. Shoman and M. S. Dhalem, "Electrically-actuated cantilever for planar evanescent tuning of microring resonators in SOI platforms," Proc. Int. Conf. Optical MEMS and Nanophotonics, Glasgow, Scotland, pp. 141-142, 2014.

[11] D. Hah and J. Bordelon, "Design of mechanically tunable optical filters with microring resonators," Proc. Design, Test, Integration and Packaging for MEMS/MOEMS, Montpellier, France, pp. 228-231, 2015.

[12] D. Hah, "A design method of comb-drive actuators for linear tuning characteristics in mechanically tunable optical filters," Microsyst. Technol., in press. doi:10.1007/s00542-015-2736-8